

**CHARACTERIZATIONS OF ZnO REINFORCED
POLY (3-HYDROXYBUTYRATE) COMPOSITES
FOR ELECTRONIC APPLICATIONS**

VISHNU CHANDAR JANAKIRAMAN

UNIVERSITI SAINS MALAYSIA

2018

**CHARACTERIZATIONS OF ZnO REINFORCED
POLY (3-HYDROXYBUTYRATE) COMPOSITES
FOR ELECTRONIC APPLICATIONS**

by

VISHNU CHANDAR JANAKIRAMAN

**Thesis submitted in fulfillment of the requirements
for the degree of
Master of Science**

January 2018

ACKNOWLEDGEMENT

I would like to express my deep appreciation to everyone who supported me during my M.Sc. studies at School of Physics, Universiti Sains Malaysia.

First and foremost, I wish to tender my profound gratitude to my main supervisor Dr. Mutharasu Devarajan for his guidance, mentorship, intellectual support, encouragements, constructive criticisms and inspiring words that really helped me to achieve outstanding goals in my research work. I feel very honored for having had the opportunity to work with him on the current thesis topic and make contribution not only to environment but also to electronic applications.

I would like to express my gratitude to my co-supervisor Dr. Azlan Abdul Aziz for his encouragements, inspiring words, wonderful attitude, and constant support which really helped me to achieve the goals throughout my studies.

I thank Dr. Shanmugan Subramani, my project coordinator for his guidance and mentorship throughout this research work. He brought to me the opportunity to work on biological, environmental, electronic applications related material science and made my research work an interdisciplinary, collaborative, and enjoyable experience.

I owe my gratitude to Murugan Paramasivan, PhD scholar and Dr. Sudesh Kumar, School of Biological Sciences, who kindly provided the polymer materials [P(3HB) homopolymer, P(3HB-*co*-10 mol% 3HHx) copolymer, P(3HB-*co*-15 mol% 3HHx) copolymer] used in this study. In addition to that, they provided testing facilities such as Differential Scanning Calorimetry (DSC), Gel Permeation Chromatography (GPC) and Tensile testing machine for my experimental and analysis work. I thank especially Murugan Paramasivan for teaching me the techniques to prepare polymer nanocomposite films, to prepare samples for GPC, DSC and tensile

experiments and for his valuable and insightful discussions on the DSC, GPC data analysis and other polymer related queries.

I gratefully acknowledge the financial support given by Universiti Sains Malaysia (USM) through USM-Fellowship Scheme for two years which really helped me to carry out this master study.

I wish to take this unique opportunity to express my great appreciation and acknowledgement to Institute of Nano-optoelectronic Research Laboratories (INOR), School of Physics, Universiti Sains Malaysia for providing the necessary facilities and excellent academic environment for a successful completion of my work. I thank the INOR staffs especially Ms. Bee Choo, Mr. Abdul Jamil Yusuf, Ms. Mahfuzah Mohamad Fuad, Mr. Mohamed Mustaqim Abu Bakar and Mr. Shahil Ahmad Khosaini for their technical support during experiments and characterizations.

I acknowledge the assistance provided by School of Chemical Sciences for the Thermogravimetric Analysis (TGA) experiment, School of Industrial Technology for pendulum hardness experiment, Communication Laboratory in School of Electronics and Communication Engineering for dielectric experiment. I thank Dr. Gan Chee Yuen, Analytical Biochemical Research Centre, Universiti Sains Malaysia (USM) for providing the facilities to do rheology experiment.

Finally, I am extremely grateful to my parents, Janakiraman Nagarathinam and Malarvizhi, and my sisters Ramya, Suganya and Kaviya for their support and love while pursuing my studies over the years.

Vishnu Chandar Janakiraman

January 2018

Universiti Sains Malaysia

TABLE OF CONTENTS

ACKNOWLEDGEMENT.....	ii
TABLE OF CONTENTS.....	iv
LIST OF TABLES.....	viii
LIST OF FIGURES.....	xi
LIST OF SYMBOLS.....	xv
LIST OF ABBREVIATIONS.....	xvii
ABSTRAK.....	xxi
ABSTRACT.....	xxiii
CHAPTER 1: INTRODUCTION.....	1
1.1 Overview of problems faced by humans due to the existing technology...	1
1.2 Introduction to biodegradable polymers and polymer composites.....	4
1.3 Problem Statement.....	5
1.4 Objectives of Research.....	8
1.5 Scope of Study.....	8
1.6 Originality of Thesis.....	9
1.7 Organization of Thesis.....	10
CHAPTER 2: LITERATURE REVIEW.....	12
2.1 Introduction.....	12
2.2 Overview of the general properties of P(3HB) homopolymer and P(3HB-co-3HHx) copolymer.....	12
2.3 Overview of the existing materials used in dielectric substrate, heat sinks, and LED encapsulation applications.....	15
2.4 Overview of blends of polymer – polymer composites.....	19
2.5 Overview of blends of polymer – nanofillers composites.....	23

2.6	Overview of ZnO based polymer composites.....	26
2.7	Polymer composites used in dielectric substrate, heatsinks LED encapsulation and other UV-related applications.....	28
2.8	Literature review summary.....	29
	CHAPTER 3: METHODOLOGY AND CHARACTERIZATIONS.....	30
3.1	Introduction.....	30
3.2	Material Section.....	30
3.3	Methodology and flow chart.....	30
3.4	Biosynthesis and extraction of pure polymers from recombinant. C. necator Re2058/pCB113.....	33
3.5	Preparation of pure polymer and polymer composite films using solution casting method.....	34
3.6	Characterization Techniques.....	35
3.6.1	X-Ray Diffraction (XRD).....	35
3.6.2	Atomic Force Microscopy (AFM).....	37
3.6.3	Field Emission Scanning Electron Microscopy (FESEM).....	37
3.6.4	Gel Permeation Chromatography (GPC).....	37
3.6.5	Differential Scanning Calorimetry (DSC).....	38
3.6.6	Thermogravimetric Analysis (TGA).....	39
3.6.7	Thermo physical parameter Analysis.....	40
3.6.8	Dielectric Analysis.....	40
3.6.9	UV-Vis Spectroscopy Analysis.....	40
3.6.10	Tensile Tests.....	40
3.6.11	Pendulum Hardness Analysis.....	42
3.6.12	Rheology Analysis.....	42

3.7	Chapter 3 conclusion.....	42
CHAPTER 4: RESULTS AND DISCUSSIONS.....		43
4.1	Introduction.....	43
4.2	X-Ray Diffraction Characterization.....	43
4.2.1	XRD Characterization – Peak Position analysis.....	43
4.2.2	XRD Characterization – Crystallite Size analysis.....	50
4.2.3	XRD Characterization – Dislocation Density analysis.....	52
4.2.4	XRD Characterization – Texture Coefficient analysis.....	54
4.3	AFM surface analysis.....	56
4.4	FESEM surface analysis.....	65
4.5	Gel Permeation Chromatography analysis.....	71
4.6	Differential Scanning Calorimetry analysis.....	75
4.6.1	Melting temperature (T_m).....	78
4.6.2	Degree of Crystallinity (X_c).....	83
4.7	Thermogravimetric analysis.....	85
4.8	Thermophysical parameter analysis.....	96
4.8.1	Thermal Conductivity analysis.....	96
4.8.2	Thermal Diffusivity analysis.....	101
4.9	Dielectric analysis.....	103
4.9.1	Dielectric analysis – Relative permittivity (ϵ').....	103
4.9.2	Dielectric analysis – Loss tangent ($\tan \delta$).....	111
4.10	UV-Vis Spectroscopy analysis.....	115
4.10.1	UV-Vis analysis – Absorption spectra.....	115
4.10.2	UV-Vis analysis – Reflectance spectra.....	122

4.11	Tensile Tests.....	127
4.11.1	Young’s modulus (E).....	127
4.11.2	Ultimate tensile strength.....	131
4.11.3	Yield strength.....	132
4.11.4	Ductility.....	134
4.12	Hardness analysis.....	136
4.13	Rheology analysis.....	139
4.14	Chapter 4 summary.....	153
	CHAPTER 5: CONCLUSION AND FUTURE WORK.....	154
5.1	Conclusion.....	154
5.2	Future work.....	155
	REFERENCES.....	157
	LIST OF PUBLICATIONS	

LIST OF TABLES

	Page	
Table 3.1	Minimal medium used for P(3HB) homopolymer, P(3HB- <i>co</i> -10 mol% 3HHx) copolymer, P(3HB- <i>co</i> -15 mol% 3HHx) copolymer preparation	33
Table 4.1	Peaks related to P(3HB) homopolymer, P(3HB- <i>co</i> -10 mol% 3HHx) copolymer, P(3HB- <i>co</i> -15 mol% 3HHx) copolymer and ZnO NPs indexed from XRD spectra	46
Table 4.2	Surface parameters of pure P(3HB) homopolymer and P(3HB)/ZnO nanocomposite film samples	61
Table 4.3	Surface parameters of pure P(3HB- <i>co</i> -10 mol% 3HHx) copolymer and P(3HB- <i>co</i> -10 mol% 3HHx)/ZnO nanocomposite film samples	62
Table 4.4	Surface parameters of pure P(3HB- <i>co</i> -15 mol% 3HHx) copolymer and P(3HB- <i>co</i> -15 mol% 3HHx)/ZnO nanocomposite film samples	63
Table 4.5	Mass-average molar mass (M_w), number-average molar mass (M_n) and molar mass dispersity (D_M) data obtained from GPC analysis for pure P(3HB) homopolymer and ZnO NPs reinforced P(3HB) composite samples	72
Table 4.6	Mass-average molar mass (M_w), number-average molar mass (M_n) and molar mass dispersity (D_M) data obtained from GPC analysis for pure P(3HB- <i>co</i> -10 mol% 3HHx) copolymer and ZnO NPs reinforced P(3HB- <i>co</i> -10 mol% 3HHx) composite samples	73
Table 4.7	Mass-average molar mass (M_w), number-average molar mass (M_n) and molar mass dispersity (D_M) data obtained from GPC analysis for pure P(3HB- <i>co</i> -15 mol% 3HHx) copolymer and ZnO NPs reinforced P(3HB- <i>co</i> -15 mol% 3HHx) composite samples	74
Table 4.8	Thermal parameters of pure P(3HB) homopolymer and P(3HB)/ZnO nanocomposite samples obtained from DSC thermograms	78
Table 4.9	Thermal parameters of pure P(3HB- <i>co</i> -10 mol% 3HHx) copolymer and P(3HB- <i>co</i> -10 mol% 3HHx)/ZnO nanocomposite samples obtained from DSC thermograms	79

Table 4.10	Thermal parameters of pure P(3HB- <i>co</i> -15 mol% 3HHx) copolymer and P(3HB- <i>co</i> -10 mol% 3HHx)/ZnO nanocomposite samples obtained from DSC thermograms	82
Table 4.11	Thermal degradation and stability parameters obtained from TGA and dTG thermograms for pure P(3HB) homopolymer and ZnO NPs reinforced P(3HB) composites	90
Table 4.12	Thermal degradation and stability parameters obtained from TGA and dTG thermograms for pure P(3HB- <i>co</i> -10 mol% 3HHx) copolymer and ZnO NPs reinforced P(3HB- <i>co</i> -10 mol% 3HHx) composites	90
Table 4.13	Thermal degradation and stability parameters obtained from TGA and dTG thermograms for pure P(3HB- <i>co</i> -15 mol% 3HHx) copolymer and ZnO NPs reinforced P(3HB- <i>co</i> -15 mol% 3HHx) composites	91
Table 4.14	Dielectric constant or relative permittivity and loss tangent of pure P(3HB) homopolymer and ZnO NPs reinforced P(3HB) composites at three critical frequencies	107
Table 4.15	Dielectric constant or relative permittivity and loss tangent of pure P(3HB- <i>co</i> -10 mol% 3HHx) copolymer and ZnO NPs reinforced P(3HB- <i>co</i> -10 mol% 3HHx) composites at three critical frequencies	108
Table 4.16	Dielectric constant or relative permittivity and loss tangent of pure P(3HB- <i>co</i> -15 mol% 3HHx) copolymer and ZnO NPs reinforced P(3HB- <i>co</i> -15 mol% 3HHx) composites at three critical frequencies	110
Table 4.17	Mechanical parameters of pure P(3HB) homopolymer and P(3HB)/ZnO nanocomposite samples	128
Table 4.18	Mechanical parameters of pure P(3HB- <i>co</i> -10 mol% 3HHx) copolymer and P(3HB- <i>co</i> -10 mol% 3HHx)/ZnO nanocomposite samples	129
Table 4.19	Mechanical parameters of pure P(3HB- <i>co</i> -15 mol% 3HHx) copolymer and P(3HB- <i>co</i> -15 mol% 3HHx)/ZnO nanocomposite samples	130
Table 4.20	Pendulum hardness of pure P(3HB) homopolymer and P(3HB)/ZnO nanocomposite samples obtained from Konig pendulum hardness tester	136
Table 4.21	Pendulum hardness of pure P(3HB- <i>co</i> -10 mol% 3HHx) copolymer and P(3HB- <i>co</i> -10 mol% 3HHx)/ZnO nanocomposite samples obtained from Konig pendulum hardness tester	137

Table 4.22	Pendulum hardness of pure P(3HB- <i>co</i> -15 mol% 3HHx) copolymer and P(3HB- <i>co</i> -15 mol% 3HHx)/ZnO nanocomposite samples obtained from Konig pendulum hardness tester	138
Table 4.23	Comparison chart of P(3HB)/ZnO, P(3HB- <i>co</i> -10 mol% 3HHx)/ZnO and P(3HB- <i>co</i> -15 mol% 3HHx)/ZnO nanocomposites obtained from different characterization used in this study	147
Table 4.24	Comparison chart of different properties of the prepared polymer composites with FR4, polyimide (kapton) for biodegradable flexible dielectric substrate applications	150
Table 4.25	Comparison chart of different properties of the prepared polymer composites with aluminium and thermoplastic materials such as polypropylene, polycarbonate, polyvinyl chloride for heat sink applications	151
Table 4.26	Comparison chart of different properties of the prepared polymer composites with silicone (OP966 HB LED silicone) for LED encapsulation applications (UV free LEDs)	152

LIST OF FIGURES

		Page
Figure 2.1	Molecular structure of poly (3-hydroxybutyrate) [P(3HB)] homopolymer	14
Figure 2.2	Molecular structure of poly (3-hydroxybutyrate- <i>co</i> -3-hydroxyhexanoate) [P(3HB- <i>co</i> -3HHx)] copolymer	14
Figure 3.1	Flow chart of the complete project – characterizations of zinc oxide reinforced poly (3-hydroxybutyrate) composites for electronic applications	32
Figure 4.1	Complete XRD spectra of pure P(3HB) homopolymer and ZnO NPs reinforced P(3HB) composite films	44
Figure 4.2	Complete XRD spectra of pure P(3HB- <i>co</i> -10 mol% 3HHx) copolymer and ZnO NPs reinforced P(3HB- <i>co</i> -10 mol% 3HHx) composite films	44
Figure 4.3	Complete XRD spectra of pure P(3HB- <i>co</i> -15 mol% 3HHx) copolymer and ZnO NPs reinforced P(3HB- <i>co</i> -15 mol% 3HHx) composite films	45
Figure 4.4	Variation in peak intensity as well as peak shifting for the XRD spectra of the characteristic peak of (a) P(3HB) homopolymer, (b) P(3HB- <i>co</i> -10 mol% 3HHx) copolymer, (c) P(3HB- <i>co</i> -15 mol% 3HHx) copolymer observed at $\sim 13.5^\circ$	48
Figure 4.5	3D AFM images of pure P(3HB) homopolymer and ZnO NPs reinforced P(3HB) composite films	58
Figure 4.6	3D AFM images of pure P(3HB- <i>co</i> -10 mol% 3HHx) copolymer and ZnO NPs reinforced P(3HB- <i>co</i> -10 mol% 3HHx) composite films	59
Figure 4.7	3D AFM images of pure P(3HB- <i>co</i> -15 mol% 3HHx) copolymer and ZnO NPs reinforced P(3HB- <i>co</i> -15 mol% 3HHx) composite films	60
Figure 4.8	FESEM images of pure P(3HB) homopolymer and ZnO NPs reinforced P(3HB) composite samples recorded at 5kx magnification	66
Figure 4.9	FESEM images of pure P(3HB- <i>co</i> -10 mol% 3HHx) copolymer and ZnO NPs reinforced P(3HB- <i>co</i> -10 mol% 3HHx) composite samples recorded at 5kx magnification	67

Figure 4.10	FESEM images of pure P(3HB- <i>co</i> -15 mol% 3HHx) copolymer and ZnO NPs reinforced P(3HB- <i>co</i> -15 mol% 3HHx) composite samples recorded at 10kx magnification	68
Figure 4.11	DSC second heating scans of pure P(3HB) homopolymer and ZnO NPs reinforced P(3HB) composite samples	76
Figure 4.12	DSC second heating scans of pure P(3HB- <i>co</i> -10 mol% 3HHx) copolymer and ZnO NPs reinforced P(3HB- <i>co</i> -10 mol% 3HHx) composite samples	77
Figure 4.13	DSC second heating scans of pure P(3HB- <i>co</i> -15 mol% 3HHx) copolymer and ZnO NPs reinforced P(3HB- <i>co</i> -15 mol% 3HHx) composite samples	77
Figure 4.14	Thermograms of pure P(3HB) homopolymer and ZnO NPs reinforced P(3HB) composite samples (a) TGA and (b)dTG	87
Figure 4.15	Thermograms of pure P(3HB- <i>co</i> -10 mol% 3HHx) copolymer and ZnO NPs reinforced P(3HB- <i>co</i> -10 mol% 3HHx) composite samples (a) TGA and (b)dTG	88
Figure 4.16	Thermograms of pure P(3HB- <i>co</i> -15 mol% 3HHx) copolymer and ZnO NPs reinforced P(3HB- <i>co</i> -15 mol% 3HHx) composite samples (a) TGA and (b)dTG	89
Figure 4.17	Thermal conductivity and thermal diffusivity of pure P(3HB) homopolymer and ZnO NPs reinforced P(3HB) composite samples	96
Figure 4.18	Thermal conductivity and thermal diffusivity of pure P(3HB- <i>co</i> -10 mol% 3HHx) copolymer and ZnO NPs reinforced P(3HB- <i>co</i> -10 mol% 3HHx) composite samples	97
Figure 4.19	Thermal conductivity and thermal diffusivity of pure P(3HB- <i>co</i> -15 mol% 3HHx) copolymer and ZnO NPs reinforced P(3HB- <i>co</i> -15 mol% 3HHx) composite samples	98
Figure 4.20	Dielectric constant or relative permittivity (ϵ') of pure P(3HB) homopolymer and ZnO NPs reinforced P(3HB) composites with respect to frequency ranging from 1MHz to 1GHz	104
Figure 4.21	Dielectric constant or relative permittivity (ϵ') of pure P(3HB- <i>co</i> -10 mol% 3HHx) copolymer and ZnO NPs reinforced P(3HB- <i>co</i> -10 mol% 3HHx) composites with respect to frequency ranging from 1MHz to 1GHz	105

Figure 4.22	Dielectric constant or relative permittivity (ϵ') of pure P(3HB- <i>co</i> -15 mol% 3HHx) copolymer and ZnO NPs reinforced P(3HB- <i>co</i> -15 mol% 3HHx) composites with respect to frequency ranging from 1MHz to 1GHz	106
Figure 4.23	Loss tangent ($\tan \delta$) of pure P(3HB) homopolymer and ZnO NPs reinforced P(3HB) composites with respect to frequency ranging from 1MHz to 1GHz	112
Figure 4.24	Loss tangent ($\tan \delta$) of pure P(3HB- <i>co</i> -10 mol% 3HHx) copolymer and ZnO NPs reinforced P(3HB- <i>co</i> -10 mol% 3HHx) composites with respect to frequency ranging from 1MHz to 1GHz	113
Figure 4.25	Loss tangent ($\tan \delta$) of pure P(3HB- <i>co</i> -15 mol% 3HHx) copolymer and ZnO NPs reinforced P(3HB- <i>co</i> -15 mol% 3HHx) composites with respect to frequency ranging from 1MHz to 1GHz	114
Figure 4.26	Absorption spectra of pure P(3HB) homopolymer and ZnO NPs reinforced P(3HB) composites with respect to wavelength ranging from 200 nm to 1000 nm	117
Figure 4.27	Absorption spectra of pure P(3HB- <i>co</i> -10 mol% 3HHx) homopolymer and ZnO NPs reinforced P(3HB- <i>co</i> -10 mol% 3HHx) composites with respect to wavelength ranging from 200 nm to 1000 nm	118
Figure 4.28	Absorption spectra of pure P(3HB- <i>co</i> -15 mol% 3HHx) homopolymer and ZnO NPs reinforced P(3HB- <i>co</i> -15 mol% 3HHx) composites with respect to wavelength ranging from 200 nm to 1000 nm	120
Figure 4.29	Reflectance spectra of pure P(3HB) homopolymer and ZnO NPs reinforced P(3HB) composites with respect to wavelength ranging from 200 nm to 1000 nm	123
Figure 4.30	Reflectance spectra of pure P(3HB- <i>co</i> -10 mol% 3HHx) homopolymer and ZnO NPs reinforced P(3HB- <i>co</i> -10 mol% 3HHx) composites with respect to wavelength ranging from 200 nm to 1000 nm	125
Figure 4.31	Reflectance spectra of pure P(3HB- <i>co</i> -15 mol% 3HHx) homopolymer and ZnO NPs reinforced P(3HB- <i>co</i> -15 mol% 3HHx) composites with respect to wavelength ranging from 200 nm to 1000 nm	126
Figure 4.32	Storage modulus (G') of pure P(3HB) homopolymer and ZnO NPs reinforced P(3HB) composites with respect to time period ranging from 0 min to 30 min	140

Figure 4.33	Storage modulus (G') of pure P(3HB- <i>co</i> -10 mol% 3HHx) copolymer and ZnO NPs reinforced P(3HB- <i>co</i> -10 mol% 3HHx) composites with respect to time period ranging from 0 min to 30 min	141
Figure 4.34	Storage modulus (G') of pure P(3HB- <i>co</i> -15 mol% 3HHx) copolymer and ZnO NPs reinforced P(3HB- <i>co</i> -15 mol% 3HHx) composites with respect to time period ranging from 0 min to 30 min	142
Figure 4.35	Loss modulus (G'') of pure P(3HB) homopolymer and ZnO NPs reinforced P(3HB) composites with respect to time period ranging from 0 min to 30 min	144
Figure 4.36	Loss modulus (G'') of pure P(3HB- <i>co</i> -10 mol% 3HHx) copolymer and ZnO NPs reinforced P(3HB- <i>co</i> -10 mol% 3HHx) composites with respect to time period ranging from 0 min to 30 min	145
Figure 4.37	Loss modulus (G'') of pure P(3HB- <i>co</i> -15 mol% 3HHx) copolymer and ZnO NPs reinforced P(3HB- <i>co</i> -15 mol% 3HHx) composites with respect to time period ranging from 0 min to 30 min	146

LIST OF SYMBOLS

\AA	Angstrom
D	Crystallite Size
$^{\circ}\text{C}$	Degree celsius
X_c	Degree of crystallinity
k	Dimensionless shape factor, constant equal to 0.94
δ	Dislocation density
β_D	Line broadening at half the maximum intensity (FWHM)
G''	Loss modulus
$\text{Tan}(\delta)$	Loss tangent/energy dissipation capacity
M_w	Mass-average molar mass
T_m	Melting temperature
T_g	Glass transition temperature
ΔH_m	Melting enthalpy
$I_a(\text{hkl})$	Measured or observed intensity used for texture analysis
D_M	Molar mass dispersity
N_2	Nitrogen gas
N	Number of diffraction peaks used for texture analysis
M_n	Number-average molar mass
θ	Peak position
%	Percentage
ϵ'	Relative permittivity or dielectric constant
ϵ	Strain
σ	Stress

s	Seconds
G'	Storage modulus
Si	Silicon
$I_a(hkl)$	Standard intensity used for texture analysis
$T_c(hkl)$	Texture coefficient
$(\Delta H_{M,PHB}^\circ)$	Theoretical melting enthalpy of 100% crystalline polyhydroxybutyrate (PHB) sample
k	Thermal conductivity
α	Thermal diffusivity
TiO ₂	Titanium dioxide
λ	Wavelength
ϕ_{ZnO}	Weight fraction of zinc oxide nanoparticles present in polymer nanocomposites
E	Young's modulus
ZnO	Zinc Oxide

LIST OF ABBREVIATIONS

AFM	Atomic force microscopy
Al	Aluminium
AR	Analytical reagents
a.u.	arbitrary unit
ASTM	American Society for Testing and Materials
BNT	Ba _{4.2} Nd _{9.2} Ti ₁₈ O ₅₄ ceramic
CR	Char residue
CNTs	Carbon nanotubes
CEM-3	Composite epoxy material – 3
Da	Dalton
dTG	Derivative of thermogravimetric analysis
DSC	Differential scanning calorimetry
esp	Endothermic shoulder peak
FWHM	Full width at half maximum
FESEM	Field emission scanning electron microscopy
FR4	Flame retardant 4
GPC	Gel permeation chromatography
GHz	Giga hertz
G	Gram
GO	Graphene oxide
HA	Hydroxyapatite
HHx	Hydroxyhexanoate
HPCF	High performance carbon fiber

K	Kelvin
LED	Light emitting diode
L	Litre
MHz	Mega hertz
MHHPA	Methylhexahydrophthalic anhydride
mL	Millilitre
μm	Micrometre
μL	Microlitre
mg	Milligram
mm	Millimetre
Min	minutes
nm	Nanometre
NPs	Nanoparticles
NR	Nutrient rich
OMMT	Organo-montmorillonite
Pa	Pascal
PBS	Polybutylene succinate
PCL	Polycaprolactone
PC	Polycarbonate
PCM	Phase change material
PDMS	Polydimethylsiloxane
PET	Polyethylene terephthalate
PHAs	Polyhydroxyalkanoates
PHB	Polyhydroxybutyrate
PHV	Polyhydroxyvalerate

PLA	Poly lactic acid
PMMA	Poly (methyl methacrylate)
PP	Polypropylene
PS	Polystyrene
PTFE	Polytetrafluoroethylene
PVC	Polyvinylchloride
PI	Polyimide
P(3HB)	Poly (3-hydroxybutyrate)
P(3HB- <i>co</i> -3HHx)	Poly (3-hydroxybutyrate- <i>co</i> -3-hydroxyhexanoate)
PHBV	Poly (3-hydroxybutyrate- <i>co</i> -3-hydroxyvalerate)
P(3HB- <i>co</i> -10 mol% 3HHx)	Poly (3-hydroxybutyrate- <i>co</i> -10 mol% 3-hydroxyhexanoate)
P(3HB- <i>co</i> -15 mol% 3HHx)	Poly (3-hydroxybutyrate- <i>co</i> -15 mol% 3-hydroxyhexanoate)
PCB	Printed circuit board
RF	Radio frequency
Recombinant <i>C. necator</i>	Recombinant <i>Cupriavidus necator</i>
RID	Refractive index detector
rpm	Revolutions per minute
SiC	Silicon carbide
TBPM	Tetrabutylphosphonium methanesulfonate
TGA	Thermogravimetric analysis
TiO ₂	Titanium di oxide
TCP	Tricalcium phosphate
UTS	Ultimate tensile strength

UV	Ultraviolet
Vis	Visible
VVM	Vessel volumes per minute
W	Watt
XRD	X-ray diffraction
ZnO	Zinc oxide

**PENCIRIAN KOMPOSIT POLY (3-HYDROXYBUTYRATE) DIPERKUAT
ZnO UNTUK APLIKASI ELEKTRONIK**

ABSTRAK

Dalam kajian ini, polimer tulen [P(3HB) homopolimer, P(3HB-*co*-10 mol% 3HHx) kopolimer dan P(3HB-*co*-15 mol% 3HHx) kopolimer] dan komposit nano [P(3HB)/ZnO, P(3HB-*co*-10 mol% 3HHx)/ZnO dan P(3HB-*co*-15 mol% 3HHx)/ZnO] filem dengan tujuh kepekatan ZnO NPs yang berbeza antara 0% hingga 30% telah dihasilkan menggunakan kaedah acuan cecair. Kesan ZnO NPs terhadap perbezaan sifat polimer tulen dan filem komposit nano telah dikaji untuk mencari potensi aplikasinya dalam bidang elektronik. Analisis XRD jelas mengesahkan kehadiran polimer [P(3HB) homopolimer, P(3HB-*co*-10 mol% 3HHx) kopolimer dan P(3HB-*co*-15 mol% 3HHx) kopolimer] dan nanopartikel ZnO (NPs). Analisis AFM dan FESEM mengesahkan permukaan licin P(3HB-*co*-15 mol% 3HHx)/ZnO komposit nano berbanding P(3HB-*co*-10 mol% 3HHx)/ZnO dan P(3HB)/ZnO komposit nano jelas menunjukkan kemungkinan kekonduksian haba yang tinggi. Analisis DSC mengesahkan suhu lebur yang tinggi P(3HB)/ZnO komposit nano (~172 °C) berkurangan dengan peningkatan kepekatan 3HHx monomer iaitu P(3HB-*co*-10 mol% 3HHx)/ZnO (~ 164 °C) dan P(3HB-*co*-15 mol% 3HHx)/ZnO (~ 159 °C) komposit nano. Analisis TGA menunjukkan tingkah laku kestabilan haba yang baik untuk komposit nano dengan menunjukkan peningkatan suhu degradasi akhir (T_f). Seperti yang dijangkakan P(3HB-*co*-15 mol% 3HHx)/ZnO komposit nano memaparkan kekonduksian haba yang lebih tinggi (10 hingga 30% peningkatan) daripada dua komposit nano lain dan menunjukkan pencapaian keseimbangan haba lebih cepat daripada komposit nano. P(3HB)/ZnO komposit nano menunjukkan pemalar dielektrik yang tinggi (~ 2.66 - 5.19) dengan kehilangan tangen <0.02 berbanding dua komposit

lain yang lebih besar daripada atau sama dengan substrat FR4. Analisis UV-Vis menunjukkan penyerapan yang kuat dalam kawasan UV oleh komposit nano berbanding polimer tulen. P(3HB)/ZnO komposit nano memaparkan modulus keanjalan yang tinggi, kekuatan tegangan yang hebat, kekuatan alah dan kekerasan daripada dua komposit lain. Analisis reologi membuktikan reaksi viskoelastik P(3HB)/ZnO komposit nano dengan simpanan yang tinggi dan kekurangan modulus daripada dua komposit nano lain. Keseluruhan P(3HB)/ZnO komposit nano akan menjadi bahan yang paling baik untuk aplikasi substrat dielektrik dan penyerap haba manakala P(3HB-co-10 mol% 3HHx)/ZnO dan P(3HB-co-15 mol% 3HHx)/ZnO komposit nano boleh dicadangkan untuk pembangunan LED bebas UV, UV dan aplikasi perlindungan NIR.

CHARACTERIZATIONS OF ZnO REINFORCED POLY (3-HYDROXUBUTYRATE) COMPOSITES FOR ELECTRONIC APPLICATIONS

ABSTRACT

In this work, pure polymer [P(3HB) homopolymer, P(3HB-*co*-10 mol% 3HHx) copolymer and P(3HB-*co*-15 mol% 3HHx) copolymer] and its nanocomposite [P(3HB)/ZnO, P(3HB-*co*-10 mol% 3HHx)/ZnO and P(3HB-*co*-15 mol% 3HHx)/ZnO] films with seven different concentration of ZnO NPs ranging from 0% to 30% were fabricated using solution casting method. The effect of ZnO NPs on different properties of pure polymer and its nanocomposite films were studied to find its potential applications in electronics field. The XRD analysis clearly confirms the presence of polymer [P(3HB) homopolymer, P(3HB-*co*-10 mol% 3HHx) copolymer, P(3HB-*co*-15 mol% 3HHx) copolymer] and ZnO nanoparticles (NPs). AFM and FESEM analysis confirmed the smoother surface of P(3HB-*co*-15 mol% 3HHx)/ZnO nanocomposites than P(3HB-*co*-10 mol% 3HHx)/ZnO and P(3HB)/ZnO nanocomposites which clearly indicated the possibility of high thermal conductivity. DSC analysis confirmed the high melting temperature of P(3HB)/ZnO nanocomposites (~ 172 °C) which decreased with increasing concentration of 3HHx monomer concentration i.e. P(3HB-*co*-10 mol% 3HHx)/ZnO (~ 164 °C) and P(3HB-*co*-15 mol% 3HHx)/ZnO (~ 159 °C) nanocomposites. TGA analysis showed good thermal stability behavior for all prepared nanocomposites by exhibiting increased final degradation temperature (T_f). As expected P(3HB-*co*-15 mol% 3HHx)/ZnO nanocomposites exhibited higher thermal conductivity (10 to 30% improvement) than other two nanocomposites and indicated the faster thermal equilibrium achievement of the prepared nanocomposites. P(3HB)/ZnO nanocomposite showed high dielectric

constant ($\sim 2.66 - 5.19$) with loss tangent < 0.02 than other two composites which is greater than or equal to FR4 substrate. UV-Vis analysis showed strong absorption in the UV region for nanocomposites compared to pure polymer. P(3HB)/ZnO nanocomposites exhibited high modulus of elasticity, ultimate tensile strength, yield strength and hardness than other two composites. Rheology analysis established the viscoelastic behavior of P(3HB)/ZnO nanocomposites with higher storage and loss modulus than other two nanocomposites. Overall P(3HB)/ZnO nanocomposites will be a most favorable material for the development of dielectric substrate and heat sink application whereas the other P(3HB-co-10 mol% 3HHx)/ZnO and P(3HB-co-15 mol% 3HHx)/ZnO nanocomposites can be suggested for the development of UV-free LEDs, UV and NIR shielding applications.

CHAPTER 1

INTRODUCTION

1.1 Overview of problems faced by humans due to the existing technology

Ecological contamination [1] and Ultraviolet (UV) radiation [2] are the most important threats faced by human species across the globe. The growth of human population continues to grow across the globe which results in the growth of industrial, urban, technological, and economic development. However, the usage of non-biodegradable petroleum based chemicals like polypropylene (PP), polycarbonate (PC), polyethylene terephthalate (PET), polyvinylchloride (PVC) and polyimide (Kapton) in industrial and non-industrial activities has been increased which led to the contamination of environment at global scale. Petro chemical plastics were widely used in food packaging, lightings, automobiles, consumer related products and many electronics applications such as Printed Circuit Boards (PCBs) etc. due to its easy modification of structure, shape, and properties [3-9]. Even though it is useful in developing the human community, the effects of these chemical in the environment or wild life is adverse and worst [10]. In order to suppress these chemical effects from the environment, researchers, and industrial experts from all around the globe has initiated the process to move towards green polymer technology i.e. the usage of biodegradable materials from renewable sources in all possible applications especially electronics applications which decides the development of future world [11, 12]. Electronics applications depends upon many components, but all the electronics applications work under one common core component i.e. Printed Circuit Boards (PCBs). These demands necessitate thinner flexible and rigid printed circuit board (PCB) substrates to be used in the electronic devices [13, 14].

The main base layer in all the electronic packaging structure is printed circuit boards (PCBs). Both thermoplastics and thermosets were used widely in the development of PCBs. Polytetrafluoroethylene (PTFE) – petroleum based material is one of the best-known thermoplastic material used in the development of high frequency PCBs and thermoset materials which involves epoxy resins gets hardened when mixed together because of chemical reactions between the epoxy resins [15]. PCBs contains resins and reinforcements which acts as a basic building blocks upon which electronic components are placed and formed into a complete electronic system. FR4 is the most widely used substrate material in most of the applications [16]. It is a composite of woven fiber glass and epoxy resin which is responsible for PCB's thickness and rigidity. Another type of substrate materials is polyimide (Kapton) based Flexi PCBs [6, 17] and composite epoxy material – 3 (CEM-3) [18]. The main problems associated with both materials (i.e. thermoplastics and thermosets) are its non-biodegradable nature. Being xenobiotic, petro chemical products are resistant to enzymatic degradation that increases its difficultness in disposal which in turn requires high energy and cost to recycle or dispose [19]. This led to the usage of green polymer (i.e. biodegradable polymer obtained from renewable sources) in the PCB development and its applications and is currently a hot research topic in both academic and industry world.

Ultraviolet (UV) is an electromagnetic radiation that can be divided into three regions such as UV-A (315 nm to 400 nm), UV-B (280 nm – 315 nm) and UV-C (100 – 280 nm). Nearly 3% of total UV radiation is only reaching the earth's atmosphere and due to the ozone depletion in stratospheric region, there is an increase in UV-B radiation that enters earth's atmosphere which not only causes skin damage, eye damage but also influence some chemical reactions that affects the light sensitive

goods such as juices, drinks, water, fruits, and vegetable when packed in petro chemical plastics [2, 20-22]. In order to avoid these problems, material with good UV absorption should be developed and the developed material should have biodegradable property.

Another source that emits UV-rays apart from natural source the sun, is Lighting industry especially Light Emitting Diode (LED) [23]. The growth of LED technology has drastically increased throughout the globe and it is widely used in displays, general lightings, aviation lighting, traffic lights, indicators etc. However, the major problems in LEDs are thermal management [24] and UV radiation emission problem [23]. The key factor in LEDs are thermal management and optical system that allows maximum amount of light to be transmitted from the diode. In order to improve the light output, silicone polymer material is widely used as an encapsulation material in the LEDs [25]. However, the main issue is LEDs do produce UV-rays, but the amount of emission is considerably low, but some industries claim that LEDs don't emit UV-rays [23]. Heat sinks are used as a thermal management product to transmit the excess heat energy emitted from LEDs without compromising the light output. Aluminium and copper based heatsinks are commonly used heatsinks in LED industry [26, 27]. Thermoplastic [28, 29] based heatsinks are recently introduced heat sinks which is growing rapidly in the current LED industry. Thermoplastic heatsink are 50% lighter than aluminium and can be easily modifiable, flexible, transformable to any complicated shaped heatsinks and reduce the cost by 20-30% whereas aluminum based heatsinks are not easily modifiable [29, 30]. However, the main issue in both the materials is its non-biodegradable nature. In order to eliminate this growing threat and to replace the petro chemical based products, there is a growing interest among

researchers and industrialists to develop a polymer material from renewable source that has biodegradable, UV -absorption, dielectric and flexibility properties.

1.2 Introduction to biodegradable polymers and polymer nanocomposites

Polyhydroxyalkanoates (PHAs), polycaprolactone (PCL) and poly lactic acid (PLA) etc. are biodegradable polymers in which 100% biodegradability is ensured only for PHAs [31]. Polyhydroxybutyrate (PHB) - first discovered from PHA family, is an aliphatic polyester and it is completely biodegradable with UV-resistance and water-insoluble properties which also exhibits properties similar to conventional plastics like polypropylene (PP) [32-35]. In order to eliminate the petrochemical or non-biodegradable products used in PCBs, heat sinks and UV-emission problems in LEDs, PHB can be used as replacement which exhibits properties such as biodegradable, UV-resistance, high melting temperature, and water-insoluble properties [32]. PHB or P(3HB) is one of the promising candidate that can be used in future electronic applications and product developments [12]. Though P(3HB) is fully biodegradable (degrades fully after few weeks in soil without forming any toxic products) and biocompatible it has some drawbacks that include brittleness, inherent rigidity, stiffness, and high production cost which limit its applications. In order to improve the physical properties such as flexibility and decrease the brittleness of P(3HB), 3-hydroxyhexanoate (3HHx) monomer is copolymerized with 3HB monomer, resulting in the formation of poly(3-hydroxybutyrate-*co*-3-hydroxyhexanoate) [P(3HB-*co*-3HHx)] copolymer. This copolymer has an increased flexibility compared to P(3HB) homopolymer [34, 36]. Increasing the percentage of 3HHx monomer (i.e. say 10 mol% of 3HHx and 15 mol% of 3HHx) further increases the flexibility of the copolymer which can be used for substrate, coating applications but at the same time decreases the melting temperature of the polymer.

The use of nanotechnology with biopolymer has increased rapidly across the researchers and industrialists from all around the globe. Polymer nanocomposites are a class of materials that has already gained a big attention among researchers both in academia and industry due to their exceptional properties, which are superior to those of the pure polymers and of the conventional composites [37-41]. Addition of nanofillers into the biopolymer results in bio-nanocomposites with enhanced properties while retaining the bio-related properties. Several approaches have been reported like blending P(3HB) homopolymer with other biopolymers and nanofillers [34].

1.3 Problem Statement

Biodegradable polymers are greatly demanding in electronics industry because of its novel properties and remarkable applications in the electronic and optoelectronic devices. Improvement in the polymer has been done by reinforcing the polymer with another biodegradable polymer or nanofillers [34]. P(3HB) homopolymer has been widely studied and analyzed all around the globe and it was widely used in food packaging applications and medical applications etc. [42-49]. However, still the biodegradable polymers especially P(3HB) homopolymer, P(3HB-co-10 mol% 3HHx) copolymer and P(3HB-co-15 mol% 3HHx) copolymer has received only a limited attention towards electronics and optoelectronics applications especially dielectric substrate in printed circuit board (PCBs), LEDs related applications, heatsinks, UV-blocker applications and NIR shielding applications. Many of the properties related to the above-mentioned applications are remain unclear.

The main aim of this project is to introduce green technology i.e. P(3HB) homopolymer, P(3HB-co-10 mol% 3HHx) copolymer and P(3HB-co-15 mol% 3HHx) copolymer - biodegradable polymer from renewable sources in the electronics

applications especially related to PCBs, LEDs and heat sink and other UV blocking applications. In the initial stage, it is impossible to replace the existing nondegradable polymer properties by the proposed biodegradable polymer completely, but it could be successful by gradual replacement and one cannot replace the existing electronics products using biodegradable polymer [P(3HB) homopolymer, P(3HB-*co*-10 mol% 3HHx) copolymer and P(3HB-*co*-15 mol% 3HHx) copolymer] completely. However, as an initialization, one can introduce biodegradable property i.e. [P(3HB) homopolymer, P(3HB-*co*-10 mol% 3HHx) copolymer and P(3HB-*co*-15 mol% 3HHx) copolymer] in the above-mentioned electronics applications.

PHB is considered as one of the promising candidate that can be used in future electronic applications and product developments [12]. The reasons for P(3HB-*co*-10 mol% 3HHx) and P(3HB-*co*-15 mol% 3HHx) are because of its flexibility, biodegradability and melting temperature. P3HB is slightly rigid with melting temperature around 170 °C which is suitable for the electronic applications especially heat sink, PCBs. But for flexible substrate and coating applications, the chosen polymer should have high flexibility at the same time the melting temperature should be maintained above 150 °C. P3HB with 5% 3HHx monomer has low flexibility but the melting temperature was greater than 150 °C whereas P3HB with 17% 3HHx monomer or greater has high flexibility but the melting temperature was lower than 135 °C [50]. P(3HB-*co*-10 mol% 3HHx) and P(3HB-*co*-15 mol% 3HHx) copolymers have required flexibility and at the same time the melting temperature was higher than 150 °C which makes it as a suitable candidate for this research. In order to improve the properties of the polymer, P(3HB) homopolymer was blended with other biopolymers and their properties were studied. However, the use of nanotechnology with biopolymer has increased rapidly and the addition of nanofillers into the biopolymer

results in bio-nanocomposites with enhanced properties while retaining the bio-related properties. The choice of suitable nanofillers has also been a major issue in the preparation of nanocomposites. Metal Oxide nanoparticles like ZnO and TiO₂ has drawn attention among researchers and industrialist due to its UV-absorption, antibacterial, non-toxic properties and especially due to low cost (compared to other high cost nanoparticles such as boron nitride, TiO₂, CNTs, graphite etc.), ZnO nanoparticles has been used in this research.

Biodegradable polymer [i.e. P(3HB) homopolymer, P(3HB-co-10 mol% 3HHx) copolymer and P(3HB-co-15 mol% 3HHx) copolymer] and ZnO NPs itself have UV absorption property. In general, most of the researchers uses only small quantity of nanoparticles (i.e. weight percentage of nanoparticles is much lower than the biopolymer weight percentage) in the biopolymer and studied their characteristics. In this work, ZnO NPs ranging from 0% to 30% were used to reinforce with P(3HB) homopolymer, P(3HB-co-10 mol% 3HHx) copolymer and P(3HB-co-15 mol% 3HHx) copolymer to prepare bio-nanocomposite films and their characteristics such as UV-absorption and reflectance, dielectric, mechanical, hardness, rheology, melting temperature, thermal stability, thermophysical, surface and structural properties were studied and analyzed in detail in order to find out its potential application possibilities and suggested whether the prepared bio-nanocomposite films can be used as replacement FR4 substrate or polyimide (Kapton) substrate based PCBs, to avoid UV-emission problems in LEDs, to develop flexible heatsinks, and to develop UV and NIR shielding applications.

1.4 Objectives of Research

The present work focusses on the preparation of pure polymer and nanocomposite films using solution casting method and confers upon the structural, surface, thermal, mechanical, rheological and dielectrical properties of these films. The objectives of the present work are as follows.

- 1) To investigate on biodegradable polymer and its nanocomposites and choose a proper polymer and nanofiller for the electronic applications.
- 2) To prepare pure polymer and nanocomposite films using P(3HB) homopolymer, P(3HB-co-10 mol% 3HHx) copolymer, P(3HB-co-15 mol% 3HHx) copolymer (350 mg to 500 mg) and ZnO NPs ranging from 0 to 30 wt%.
- 3) To characterize and analyze the prepared pure and biopolymer nanocomposite films.
- 4) To compare all properties and suggest the suitable polymer and its nanocomposites for the potential future applications such as
 - Biodegradable heat sinks for LED applications
 - Flexible dielectric substrates for the replacement of FR4 and Kapton based PCB applications
 - LED encapsulation for UV-free LEDs, UV and NIR shielding coating applications.

1.5 Scope of study

The scope of study lies in the usage of three different biodegradable polymers P(3HB) homopolymer, P(3HB-co-10 mol% 3HHx) copolymer and P(3HB-co-15 mol% 3HHx) copolymer which is not widely used or suggested in the development of electronics and optoelectronics applications. The main scope lies in the preparation of

pure polymer and nanocomposite films using P(3HB) homopolymer, P(3HB-*co*-10 mol% 3HHx) copolymer and P(3HB-*co*-15 mol% 3HHx) copolymer under various ZnO NPs concentrations ranging from 0% to 30% (7 different concentrations) and to investigate the effect of ZnO NPs on the structural, surface, thermal, thermophysical, mechanical, dielectric, and rheological properties of pure polymer and nanocomposites. Furthermore, the obtained properties were compared and analyzed in detail between the three polymers in order to find out its potential application possibilities and suggested whether the prepared bio-nanocomposite films can be used as replacement for FR4 substrate or polyimide (Kapton) substrate based PCBs, to develop UV-free LEDs (i.e. to avoid UV-emission problems in LEDs), to develop biodegradable and flexible heatsinks, and to develop other UV and NIR shielding applications.

1.6 Originality of thesis

Since there is no work or suggestions involving P(3HB) homopolymer, P(3HB-*co*-10 mol% 3HHx) copolymer and P(3HB-*co*-15 mol% 3HHx) copolymer in the LED encapsulation, heatsinks and PCB applications, in this work an attempt is made to prepare pure polymer and nanocomposites films using the above-mentioned polymers and ZnO NPs as a nanofiller with 7 different concentrations ranging from 0% to 30%. The films were prepared using solution casting method using chloroform as a solvent. A comparison between different properties related to the above-mentioned applications such as surface, thermal, dielectric, UV, thermal conductivity, mechanical and rheology of the prepared pure and nanocomposite films has been made since there is no discussion involving the above mentioned three polymers related to LED encapsulation, heatsinks and PCB applications in the previous studies.

1.7 Organization of thesis

The **chapter 1** of this thesis deals with the introduction and objectives of the present research work. This chapter gives the overview of the issues and highlights the problems faced by the humans due to the existing technology. Furthermore, objectives of the research work, scope of thesis and originality of thesis are described in this chapter.

The **chapter 2** contains the brief literature review about the blends of polymer - polymer composites, polymer – nanofiller composites, and ZnO based polymer composites and their properties. It also deals with brief literature review of the polymer composites used in the dielectric substrate applications, LED encapsulations, and heatsinks. Apart from that it also contains the general properties and requirements for the electronic applications especially the dielectric substrate application, LED encapsulations and heatsinks.

The **chapter 3** contains materials used in the preparation of pure polymer and nanocomposite films. It also contains the brief methodology of the preparation of polymers and the procedure to prepare the pure polymer and nanocomposite film samples. The complete characterization and its experimental procedure used in this work have been described in detail in chapter 3.

The **chapter 4** contains the complete results and discussions on the characterization of pure polymer and nanocomposite film samples. It contains the complete investigation on effect of ZnO NPs on the structural, surface, thermal, thermophysical, mechanical, dielectric and rheological properties of pure polymer and nanocomposites. Furthermore, it also discusses the applications of the prepared nanocomposite films whether it can be used as replacement for FR4 substrate or polyimide (Kapton) substrate based PCBs, to develop UV-free LEDs, to develop

biodegradable and flexible heatsinks, and to develop UV and NIR shielding applications.

The **chapter 5** deals with the conclusion obtained from the present work and its future work. Overall the results obtained have been summarized in this chapter.

CHAPTER 2

LITERATURE REVIEW

2.1 Introduction

This chapter deals with the brief literature review about biopolymer, composites and its properties and applications. This chapter has been divided into seven parts. The first part deals with the general properties of P(3HB) homopolymer and P(3HB-*co*-3HHx) copolymer. The second part deals with the analysis of basic requirement of PCBs, heat sinks, LED encapsulation applications and it covers the brief review of the existing materials used in these applications. The third part deals with brief literature review of the blends of polymer - polymer composites and its properties and applications, the fourth part consists of the literature review of polymer – nanofiller composites and its properties and applications. The fifth part deals with ZnO based polymer composites, its properties, and applications. The sixth part contains the brief literature review of the polymer composites used in the dielectric substrate applications, LED encapsulations and heatsinks applications respectively whereas the seventh and final part deals with the conclusion of literature review.

2.2 Overview of the general properties of P(3HB) homopolymer and P(3HB-*co*-3HHx) copolymer

In order to fulfill this objective, it is very important to understand the complex inter-relationships among processing, structure, composition, and properties of PHB and it is known that these relationships play an important part in the use of PHB [51, 52]. In this section, the general properties of P(3HB) homopolymer and the effects of different 3HHx monomer concentrations in the P(3HB) homopolymer is discussed here.

Poly (3-hydroxybutyrate) P(3HB) or (PHB) was first discovered from PHA family, is an aliphatic polyester which exhibits properties such as biodegradable, biocompatible, renewable, sustainable, non-toxic, UV-resistance, high melting temperature. It degrades fully after few weeks in soil without forming any toxic products and also exhibits properties similar to commercially available thermoplastics like polypropylene (PP), a tough robust material [32-35]. In addition, it has better heat resistance and water resistance compared to other biodegradable polymers such as starch and polylactic acid (PLA) [53]. The processing of P(3HB) homopolymer generally requires converting the solid raw material into a solvable form or melt form which can be done by identifying the proper solvent or thermal input such as melting temperature and heat of fusion which can be determined by the thermal properties of the P(3HB) homopolymer. Then the conversion of melt form to a solid product completely rely on the crystallization temperature and enthalpy. The property of the final solid product depends on the morphology which in turn depends on the processing mechanism [54-56].

Though P(3HB) is biodegradable, biocompatible and has many advantageous properties, it has also some drawbacks that includes brittleness, inherent rigidity, narrow thermal processing window [57] and high production cost [58] which limit its applications. In order to improve the physical properties such as flexibility and decrease the brittleness of P(3HB), 3-hydroxyhexanoate (3HHx) monomer is copolymerized with 3HB monomer, resulting in the formation of poly (3-hydroxybutyrate-*co*-3-hydroxyhexanoate) [P(3HB-*co*-3HHx)] copolymer. The molecular structure of poly (3-hydroxybutyrate) [P(3HB)] and poly (3-hydroxybutyrate-*co*-3-hydroxyhexanoate) [P(3HB-*co*-3HHx)] copolymer was shown in Fig. 2.1 and Fig. 2.2 respectively [59]. The resultant copolymers are expected to

have high flexibility, faster degradation and low melting temperature compared to P(3HB) homopolymer [34, 36]. The mechanical and physical properties of the polymer vary with respect to the concentration of copolymer [60-62]. Shimamura *et al.* [50] found that the melting temperature (T_m) of P(3HB-co-3HHx) copolymer was decreased from 177 to 130 °C as the concentration of 3HHx monomer increased from 0 to 17 mol%. Similarly, the glass transition temperature (T_g), XRD crystallinity and enthalpy of fusion (ΔH_m) were also decreased with increasing concentration of 3HHx monomer. The decrease in the crystallinity may be due to the presence of 3HHx monomer unit which indicates that 3HHx monomer cannot crystallize in the sequence of 3HB units and act as defects in the P(3HB) crystal lattice.

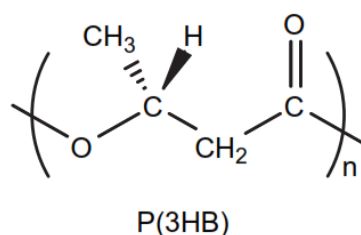


Figure 2.1 Molecular structure of poly(3-hydroxybutyrate) [P(3HB)] homopolymer

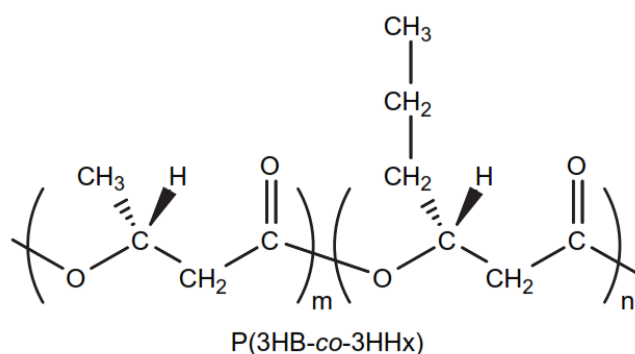


Figure 2.2 Molecular structure of poly (3-hydroxybutyrate-co-3-hydroxyhexanoate) [P(3HB-co-3HHx)] copolymer

The thermal and mechanical properties of P(3HB) homopolymer and [P(3HB-co-3HHx)] copolymers are summarized in this section. The melting temperature of P(3HB) homopolymer and glass transition temperature of P(3HB) homopolymer is

around 177 °C and 4 °C respectively [50, 63]. Doi *et al.* [64] increased the concentration of 3HHx monomer from 0 to 25 mol% and observed that the melting temperature (T_m) got decreased from 178 °C to 52 °C, T_g got decreased from 4 °C to -4 °C, ΔH_m got decreased from 97 J g⁻¹ to 19 J g⁻¹ respectively. Asrar *et al.* [65] also analyzed the thermal properties of P(3HB-*co*-3HHx) copolymer by increasing the concentration of 3HHx monomer from 2.5 to 35 mol% and found a similar trend like the above results. Doi *et al.* [64] also studied the mechanical parameters of P(3HB) homopolymer and P(3HB-*co*-3HHx) copolymer (0 to 17 mol%) and reported that the observed tensile strength of P(3HB) homopolymer was around 43 MPa whereas the addition of 3HHx monomer concentration decreased the tensile strength from 43 MPa to 20 MPa. Elongation at break for P(3HB) homopolymer was around 5% whereas the addition of 3HHx monomer increased the elongation at break value from 400 to 850% (10 to 17 mol%). Asrar *et al.* [65] also found a similar trend for tensile strength whereas for elongation at break, the observed value was around 40% for 9.5 mol% 3HHx monomer concentration which may be due to the different processing techniques used by Doi (solvent casted films) and Asrar (thermal processed films). Luo *et al.* [66] added a nucleation agent phenylalanine to P(3HB-*co*-3HHx) copolymer (13.5 mol%) and found that the addition of nucleation agent does not change the tensile strength and elongation at break values. The addition of 3HHx monomer in P(3HB) decreased the aging process and brittleness.

2.3 Overview of the existing materials used in dielectric substrate, heat sinks, and LED encapsulation applications

This section deals with the analysis of basic requirement of PCBs, heat sinks, LED encapsulation applications and it covers the brief review of the existing materials used in these applications.

The dielectric substrates should have the following general properties such as dielectric constant with low dielectric loss typically less than or equal to 0.001, fine surface finish, low temperature coefficient, uniform thickness, dimensional stability, mechanical stability, high thermal conductivity [67, 68]. FR4 substrate is one of the commonly available low-cost dielectric substrate for antenna applications and many other electronic circuit developments. Different antenna structures such as square patch antenna [69], circular disc monopole antenna [70], microstrip antenna [71], inverted-F patch antenna [72], slot antenna [73], coplanar antenna [74], dipole antenna [75] have been printed on FR4 substrates and used in microwave applications. Another application is the usage of FR4 substrate in printed circuit board (PCB). Other than FR4 substrate, material such as CEM 1-5, PTFE, Alumina were used in the PCB applications [76]. Polyimide or kapton were widely used as flexible substrates [77].

Heat sinks are an electronic component which is used to disperse the heat from the electronic components into the surrounding medium and cools it for improving the performance, reliability, premature failure of the component. The heat sinks should have the following general properties such as high thermal conductivity, thermal stability, low thermal resistance, high melting temperature for proper thermal management. All these properties depend on the selection of material. It is clear that material with high thermal conductivity can reduce thermal resistance of the heat sink well. The most common material used in heat sink application is aluminium or aluminium alloys which exhibit thermal conductivity around 200 W/mK [78]. It can be further improved by using copper which exhibit thermal conductivity around 400 W/mK [78] however because of its cost and weight it is not a justifiable material that can be used in heat sink applications. Natural graphite composite material is a material that's gaining popularity with heat sink producers nowadays. It's not as conductive as

copper, but it exhibits thermal conductivity around 370 W/mK with just 70 percent of the weight of aluminum [79]. Ekpu *et al.* [80] reviewed about the materials used for heat sinks in laptop computers and found that instead of aluminium and copper based heat sinks, an advanced composite material (Al/SiC) which exhibit superior property potentials is recommended as an optimum material for laptop computer heat sinks. Other composite materials such as copper-tungsten pseudo alloy, Dymalloy (diamond in copper-silver alloy matrix) [81], and E-Material (beryllium oxide in beryllium matrix) were often used as substrates for chips which automatically dissipates the heat from the chips. Kerns *et al.* [81] developed a copper – diamond composite which consists of type 1 diamond powder in a copper matrix that exhibits thermal conductivity around 420 W/mK which can be used as a substrate for high power density electronic components. Hong *et al.* [82] investigated the effects of open-cell aluminium foams on the performance of aluminium foam-phase change material (PCM) heat sinks in which paraffin was used as a phase change material and found that both the heating and cooling times of the copper block increases with increase in the surface area density of foams.

Thermoplastics is another type of material used in the development of heat sink because of its light weight, low cost compared to aluminium and copper, efficient, flexible, easily processable into different shapes, improved manufacturing etc. Injection molding cost of thermoplastics is lower than the metals and has higher production efficiency. The thermal conductivity of unfilled plastics is usually lower (The normal range of polymers is from 0.17 to 0.35 W/mK) [83], and a proper filler needs to be added in the plastic matrix to make it as a thermally conductive plastic which should exhibit minimum thermal conductivity of about 1 W/mK. Here are some of the thermally-conductive plastics such as polyimide + graphite 40% (1.7 W/mK),

Rubber + Al flakes (1 W/mK), commercially available electrically non-conductive plastics (1-10 W/mK), commercially available electrically conductive plastics (5-100 W/mK), epoxy + high performance carbon fiber (300 W/mK) [83].

Encapsulation materials for light emitting diodes (LEDs) generally need high thermal stability to resist yellowing, which would decrease transparency and thus ultimately reduce the light extraction efficiency. In addition to that, for high efficiency light extraction from a LED, encapsulation material should have a high refractive index which would improve the illumination performance of the LEDs. The smaller the difference in refractive index the less light is lost to internal reflection in the chip increasing the light output efficacy of the LED device. Polysiloxanes or silicone for LED encapsulant have been reported to exhibit high thermal stability [84–86]. The silicone encapsulant should have the following general properties such as high thermal conductivity, thermal stability, UV-resistance, chemical resistance, humidity and water resistance, resistance to fungus growth, high melting temperature, flexible, transparent for proper light output.

Bae *et al.* [87] prepared an ultraviolet (UV) transparent, stable methylsiloxane material by using a facile sol-gel method and used as an UV-LED encapsulant, which exhibited long-term UV stability under light soaking in UVB (~300 nm) for 1000 hours. It also showed a comparable transmittance to polydimethylsiloxane (PDMS) in the UVB (~300 nm) region as shown in Fig. 7. Kim *et al.* [88] reported a thermally stable transparent sol-gel based polysiloxane LED encapsulation material with high refractive index. The obtained materials showed excellent optical transparency with high refractive index ($n = \sim 1.56$). The transparency in the visible range was maintained even after thermal aging at 200 °C in air for 1152 hours. The same author prepared a methacrylate hybrid based on methacrylate based resins and found that the

fabricated hybriders are optically transparent and have a high refractive index of 1.565 [89]. Wu *et al.* [90] studied the thermal and optical properties of epoxy/phenyl siloxane hybrid prepared by polymerization and sol-gel condensation reactions. The refractive index of the prepared hybrid was around 1.66 – 1.70 and transmittance were around 90% in the visible wavelength. Thermal aging test slightly decrease the transmittance and refractive index by 20% and 5% respectively. Yang *et al.* [91] successfully fabricated a Cycloaliphatic epoxy hybrid bulk by thermal curing of cycloaliphatic epoxy oligosiloxane resin synthesized by a sol-gel condensation reaction with methylhexahydrophthalic anhydride (MHHPA) and tetrabutylphosphonium methanesulfonate (TBPM). The composition of MHHPA and TBPM in the resin was optimized to reduce the yellowness of the cycloaliphatic epoxy hybrid. It can be used as a LED encapsulant for white LEDs on the basis of its high thermal stability with appropriate hardness and a high refractive index of 1.55. Zhao *et al.* [92] prepared a novel polysiloxane with self-adhesion ability and higher refractive index and characterized. It has been found that the prepared curable resin has high refractive index, transparency, thermal stability, hardness, as well as good adhesive strength which can be used as an encapsulant for LEDs. In all these cases, the existing material used for the development of these applications are not biodegradable which contaminates the environment globally. In order to avoid these, scientists are moving towards green polymer i.e. the usage of biodegradable polymer derived from renewable resources in these applications.

2.4 Overview of blends of polymer – polymer composites

In order to improve the performance and to reduce the cost of the polymers, several approaches have been reported like blending of one biodegradable polymer with another polymer will expand its range of applications and offers more scope.

P(3HB) and PCL are biodegradable polymers synthesized from renewable resources and is one of the most widely studied blends [34] Lovera *et al.* [93] prepared high molecular weight polyhydroxybutyrate (PHB)/poly(ϵ -caprolactone) (PCL) and PHB/low molecular weight chemically modified PCLs (mPCL) blends by solution blending technique and studied their morphology, crystallization, and enzymatic degradation of the blends and found that high molecular weight blends were not immiscible in the entire composition range. Duarte *et al.* [94] also analyzed the (PHB)/poly(ϵ -caprolactone) (PCL) blend and discussed the thermal and mechanical behaviour of the blends prepared using injection molding method. Garcia *et al.* [95] also discussed the miscibility, mechanical and thermal properties of PHB/PCL blends prepared by twin screw co-rotating extruder and injection molding and the obtained results showed that PCL acts as an impact modifier which means that the ductility and flexibility increases with increase in the concentration of PCL in PHB/PCL blends.

Gassner *et al.* [96] investigated the composition range of compression molded sheets of PHB blended with PCL and found that PHB and PCL are immiscible, and its mechanical properties varies with respect to composition. Zhang *et al.* [97] investigated the morphology and hydrolytic behaviour of PHB/PCL, PHB/PLA, PLA/PCL blends and found that both morphology and hydrolytic behaviour depends upon the composition of the blends. Aoyagi *et al.* [98] investigated the thermal degradation properties of PHB, PCL and PLA under isothermal and non-isothermal condition. Hinuber *et al.* [99] investigated the thermal and mechanical properties of PHB/PCL blend prepared by melt extrusion method and found that the blends of PHB/PCL are promising for the applications in tissue engineering. Kil'deeva *et al.* [100] found that the same PHB/PCL blend can also be used in the preparation of biodegradable wound coverings. Dos *et al.* [101] investigated the biodegradability of

PHB/PCL blend prepared by compression method before and after irradiation and found that the rate of degradation was directly proportional to the soil alkalinity. Chee et al. [102] performed the viscometric analysis on PHB/PCL blends and demonstrated that PHB is immiscible with PCL.

Sevastianov *et al.* [103] found that both PHB and PHBV films can be used in the biomedical applications. Avella *et al.* [104] investigated the miscibility, morphology, mechanical behaviour of PHB/poly (3-hydroxybutyrate-hydroxyvalerate) (PHBV) composites and found that microstructure of the blends is regarded as an important factor in controlling the biodegradation and mechanical properties. Sombatmankhong *et al.* [105] prepared the PHB/PHBV blend using electrospinning on a stationary collector and home-made rotating cylindrical collector and found that improvement in tensile strength and elongation at break was observed for blends over those of pure ones. Sombatmankhong *et al.* [106] also prepared the PHB/PHBV blend using electrospinning technique and found that their 50/50 PHB/PHBV blend can be used for potential use as bone scaffolds.

Zhang *et al.* [107] investigated the miscibility, crystallization, and morphology of PHB/ poly(d,l-lactide) (PLA) blends and found that the thermal history caused a depression in the melting point and a decrease in crystallinity of PHB in the blends. Similarly, Abdelwahab *et al.* [108] prepared a blend of PHB (25%)/PLA (75%) with a polyester plasticizer at two different concentration (5% and 7%) and investigated its thermal, mechanical and biodegradability. Gogolewski *et al.* [109] studied the tissue response and molecular stability of the injected molded PLA, PHB, and PHBV polymer and found that all the polymers were well tolerated by tissue and shows no acute inflammation, abscess formation or tissue necrosis. Vogel *et al.* [110, 111] prepared the PHB/PLA blend and studied their structural information on a molecular

level and mechanical elongation orientation using FTIR spectroscopy imaging technique. Arrieta *et al.* [112] prepared the blends of PHB/PLA with cellulose nanocrystals (CNCs) in order to improve the properties and the reported results showed that CNCs not only increased the crystallinity but also improved the processability and thermal stability. The same PHB/PLA blend has been plasticized with natural terpene d-limonene (LIM) and found that the added plasticizer improved the thermal, barrier, mechanical properties and hence the prepared films can be used for food packaging applications [113].

Over the past few years, PHAs, particularly poly 3-hydroxybutyrate (PHB), copolymers of 3-hydroxybutyrate (P3HB-*co*-HB) and 3-hydroxyvalerate (PHBV), copolymers of 3-hydroxybutyrate and 3-hydroxyhexanoate (PHBHHx) and poly 3-hydroxyoctanoate (PHO) and its composites have been used to develop medical devices such as dressings, sutures, repair patches and devices, cardiovascular patches, orthopedic pins, stents, guided tissue repair/regeneration devices, nerve guides, cartilage and tendon repair devices, bone marrow scaffolds etc. [114] but there is no literature on electronics applications especially related to LEDs and heat sinks. Nerkar *et al.* [115] reported about the blends of PHB with an elastomeric medium-chain-length poly-3-hydroxyalkanoate (MCL-PHA) which contains 98 mol% 3-hydroxyoctanoate and 2 mol% 3-hydroxyhexanoate (also referred as PHO), prepared by melt compounding and found that the addition of PHO improved the thermal stability and tensile strain and reduced the crystallinity. Jing *et al.* [116] prepared the blend of PHBHHx/PCL and investigated its mechanical properties and found that PHBHHx/PCL blend showed improved ductility, yield strain and crystallinity.

2.5 Overview of blends of polymer – nanofiller composites

The reinforcement of nanofillers in the biopolymer resulted in polymer nanocomposites which not only improves the properties of the composites but also retains its bio related properties. This review covers the brief literature of nanofillers such as organo-montmorillonite (OMMT), carbon nanotubes (CNTs), hydroxyapatite (HA), graphite, ZnO. The factors that affects the properties of the polymer composites are usage of different fillers, filler size i.e. nano or micron, aspect ratio, specific surface area, filler dispersion and distribution, dispersion methodology i.e. mechanical stirrer or homogenizer, filler interaction inside the polymer matrix and agglomeration [117, 118]. Any small changes in these factors will affect the properties of the prepared polymer composites.

Lim *et al.* [119] prepared the blends of PHB and organo-montmorillonite (OMMT) via solvent casting method and found that the thermal stability of PHB/OMMT nanocomposites got increased with OMMT content, except for high OMMT concentration. Erceg *et al.* [120] prepared the PHB/OMMT nanocomposites using solution intercalation method and investigated the thermal stability and kinetic parameters of the non-isothermal degradation of PHB/OMMT nanocomposites. The prepared PHB/OMMT nanocomposites also showed improved thermal stability due to the addition of OMMT content. Erceg *et al.* [121] also studied the thermal stability and kinetic parameters of the isothermal degradation of PHB/OMMT nanocomposites and found that the addition of OMMT increases the thermal stability of PHB especially the addition of 7 wt% of OMMT has pronounced effect than other concentrations. Tianying *et al.* [122] investigated the kinetic parameters of isothermal crystallization of PHBV/OMMT nanocomposites and found that the presence of OMMT particles enhance the crystallization rate of PHBV and improve the isothermal crystallization

behaviour of PHBV. Prakashan *et al.* [123] prepared the PHB/OMMT nanocomposites with OMMT concentration up to 7 wt% and found that PHB reinforced with OMMT showed increased tensile, flexural, impact strength and thermal stability than pure PHB. Iggui *et al.* [124] investigated the biodegradability of PHBV/OMMT nanocomposites and confirmed the biodegradability by surface erosion and significant decrease in the molecular weight was also observed. Similarly, Correa *et al.* [125] investigated the effect of acetyl tributyl citrate plasticizer in PHB/OMMT nanocomposites and confirmed that addition of plasticizer improved processability and does not influence the nano-sized load dispersion state.

Yun *et al.* [126] prepared the nanocomposite films of PHB, PHO and single walled carbon nanotubes (SWCNTs) and studied the effect of SWCNTs on mechanical and crystallization behaviour and found that the addition of SWCNTs clearly improves the hardness and young's modulus. Yun *et al.* [127] also prepared the PHB/SWCNTs and PHO/SWCNTs using spray dying method and found that this technique is suitable for the production of bulk carbon composite fabrication. Xu *et al.* [128] prepared the PHB/ multi-walled carbon nanotubes (MWCNTs) and studied its non-isothermal melt crystallization and subsequent melting behaviour. Xu *et al.* [129] also studied the crystallization and thermal behaviour of PHB/MWCNTs and found that MWCNTs also enhances the crystallization of PHB and also improves the thermal stability of the PHB/MWCNTs nanocomposites. Huh *et al.* [130] studied the effects of carbon nanotubes on the structure and properties of PHB/MWCNTs and compared with acid treated MWCNTs (MWCNT-COOH). It is clear that the alkylated MWCNTs strengthened the PHB composites effectively than the non-alkylated MWCNTs. Liao *et al.* [131] prepared the PHB/MWCNTs using melt bending method and found that PHB/MWCNTs nanocomposites demonstrated significant improvement in thermal